Available online at www.sciencedirect.com
ScienceDirect
Physics Letters A 363 (2007) 282–289
PHYSICS LETTERS A
www.elsevier.com/locate/pla

Bursting neurons with coupling delays

Nikola Burić [a,*], Dragana Ranković [b]

[a] *Institute of Physics, PO Box 57, 11001 Belgrade, Serbia*
[b] *Department of Physics and Mathematics, Faculty of Pharmacy, University of Belgrade, Vojvode Stepe 450, Belgrade, Serbia*

Received 12 August 2006; accepted 8 November 2006

Available online 27 November 2006

Communicated by A.R. Bishop

Abstract

A pair of Hindmarsh–Rose neurons with delayed coupling is studied. Bifurcations due to time-lag and coupling and stability of the stationary state that corresponds to the quiescence behavior are analyzed. Bursting is created by coupling and its properties strongly depend on the time-lag. In particular, there is a domain of values of time-lags which renders the bursting of the two neurons exactly synchronous.

PACS: 02.30.Ks; 05.45.Xt

1. Introduction

In modeling realistic neuronal networks it is useful and also important to use explicitly the time-delays in the description of the transfer of information between the neurons. This enables us to model a complicated succession of processes that take place in real synapses by a single interaction term with an explicit time-lag in the dynamical equations of the interacting neurons. On the other hand it is known that values of the time-lag in a realistic domain can change the qualitative properties of dynamics: introduce or destroy stable oscillations and enhance or suppress synchronization between different units.

Phenomena of suppression of oscillations and synchronization are important in understanding the physiology of neuronal systems, and have been intensively studied using simple neuronal models with delayed coupling. Motivation for such studies and an extensive list of relevant references can be found in [1], and shall not be repeated here. In order to concentrate on the properties of the network connectivity most of these studies use oversimplified models of neurons. In our previous investigation [1,3,4] we have used two-dimensional representatives of type I or type II excitable systems [2] with delayed electric or chemical coupling. Such two-dimensional models of a neuron can display stationary or oscillatory dynamics but in order to model a more complicated behavior, like chaotic bursting and spiking, which is observed in real neurons, requires at least one more variable. The minimal model of bursting behavior, in real neurons requires three variables and is of the form of the Hind–Rose (HR) equations [5–7] given by

$$\dot{x} = y + 3x^2 - x^3 - z + I, \qquad \dot{y} = 1 - 5x^2 - y, \qquad \dot{z} = -rz + rS(x + 1.6), \tag{1}$$

where x is the membrane potential, y represent the fast current, like Na^+ or K^+ and z corresponds to the slow current, for example Ca^+. Slow oscillations of z variable drive the fast subsystem (x, y) through periods of oscillatory and quiescent behavior.

The constant parameter I in the model (1) represents the external current and is the bifurcation parameter, determining its qualitative behavior. When $I = 0$ there could be only one stable solution of (1) and it corresponds to the stable quiescence behavior of the neuron. However, for constant I in a certain domain away from zero the model (1) describes chaotic bursting, i.e. a series of

* Corresponding author.
E-mail address: buric@phy.bg.ac.yu (N. Burić).

0375-9601/$ – see front matter
doi:10.1016/j.physleta.2006.11.032

spikes which are chaotically interspersed with the refractory period and quiescence behavior [8]. There are some recent studies [9] of synchronization between delayed coupled HR neurons with constant I in the domain corresponding to the bursting dynamics of each isolated unit. They concentrate on the question of synchronization, and show that the time-delay can enhance the synchronization of bursting introduced by external currents. However, it is also interesting to analyze the possibility to introduce the bursting using only the time-delayed synaptic interaction between the neurons with no external current. In this case the properties of bursting of each neuron and of the synchronization between the neurons depend only on the coupling and the time-lag. In this Letter we shall study the bifurcations of the stationary solutions and synchronization of bursting which occur only due to the delayed coupling, so that in what follows $I = 0$ always. Thus, we shall analyze an isolated system of delayed coupled HR neurons.

Our Letter is organized as follows. Section 2 is devoted to the bifurcation analyzes of the stationary solution of the delayed coupled pair of HR neurons due to varying coupling strength and time-lag. In Section 3 we study the dependence of the frequency of bursts on the coupling and the time-lag, and the synchronization of bursting introduced by time-lag. Section 4 presents a summary and discussion our results.

2. Bifurcations of the stationary solution

Our aim in this section is to analyze stability of the stationary solution that corresponds to the quiescent behavior of a pair of delayed coupled HR neurons, given by the following delay-differential equations (DDE):

$$\begin{aligned}
&\dot{x}_1 = y_1 + 3x_1^2 - x_1^3 - z_1 + c\big(x_1 - x_2^\tau\big), \qquad \dot{y}_1 = 1 - 5x_1^2 - y_1, \qquad \dot{z}_1 = -rz_1 + rS(x_1 + 1.6),\\
&\dot{x}_2 = y_2 + 3x_2^2 - x_2^3 - z_2 + c\big(x_2 - x_1^\tau\big), \qquad \dot{y}_2 = 2 - 5x_2^2 - y_2, \qquad \dot{z}_2 = -rz_2 + rS(x_2 + 1.6),
\end{aligned} \tag{2}$$

where $x^\tau(t) = x(t-\tau)$, c is the coupling constant and τ is the time-lag. The coupling between the neurons is in the form of the electrical coupling. Let us first briefly recapitulate the main facts about an isolated HR neuron.

2.1. Single HR unit

An isolated HR neuron is described by the following equations

$$\dot{x} = y + 3x^2 - x^3 - z, \qquad \dot{y} = 1 - 5x^2 - y, \qquad \dot{z} = -rz + rS(x + 1.6). \tag{3}$$

Parameters r and S shall always be fixed to the values $S = 4$, $r = 0.0021$, which are common in the analyzes of the bursting behavior. As pointed out, the bursting is possible only if an external current is added to the system (3), like in (1), but in our case $I = 0$, and the bursting will appear due to the coupling with another neuron.

The system (3) has only one real stationary solution:

$$(x_0, y_0, z_0) = (-1.60453, -11.8726, -0.01812). \tag{4}$$

After the transformation $x \to x - x_0$, $y \to y - y_0$, $z \to z - z_0$ the linearized part of (1) is

$$\dot{x} = \big(6x_0 - 3x_0^2\big)x + y - z, \qquad \dot{y} = -10x_0x - y, \qquad \dot{z} = 4rx - rz. \tag{5}$$

The characteristic equation of (5) is

$$(\lambda + r)(\lambda + 1)(\lambda + 3x_02 - 6x_0) + 4r(\lambda + 1) + 10x_0(\lambda + r) = 0. \tag{6}$$

Substitution of the particular values of x_0 and r gives a third order polynomial with solutions:

$$\lambda_1 = -18.2783, \qquad \lambda_2 = -0.0645022, \qquad \lambda_3 = -0.00344365. \tag{7}$$

Thus, the stationary solution (3) is a stable node, for the chosen values of the parameters.

2.2. Coupled pair of HR unit

Let us now consider the stability of the stationary solution of the full system (2) for varying values of $c > 0$ and $\tau > 0$ and for fixed values of the parameters $S = 4$, $r = 0.0021$.

The stationary solution that corresponds to the quiescent state of the two neurons is given by

$$x_1 = x_2 = x_0, \qquad y_1 = y_2 = y_0, \qquad z_1 = z_2 = 0, \tag{8}$$

where (x_0, y_0, z_0) are given by (4), and is independent of c.

Shifting the coordinates so that the stationary solution is at the origin and linearization of the system (2) results in

$$\begin{aligned}
&\dot{x}_1 = \big(6x_0 - 3x_0^2\big)x_1 + y_1 - z_1 - cx_2^\tau, \qquad \dot{y}_1 = -10x_0x_1 - y_1, \qquad \dot{z}_1 = 4rx_1 - rz_1,\\
&\dot{x}_2 = \big(6x_0 - 3x_0^2\big)x_2 + y_2 - z_2 - cx_1^\tau, \qquad \dot{y}_2 = -10x_0x_2 - y_2, \qquad \dot{z}_2 = 4rx_2 - rz_2.
\end{aligned} \tag{9}$$

The characteristic equation can be factored into the form

$$\Delta_1(\lambda)\Delta_2(\lambda) = 0,$$
$$\Delta_{1,2}(\lambda) = (\lambda+1)(\lambda+2)(\lambda+3x_0-6x_0-c)+4r(\lambda+1)+10x_0(\lambda+2) \pm c(\lambda+1)(\lambda+2)\exp(-\lambda\tau). \tag{10}$$

2.3. Instantaneous coupling $\tau = 0$

To worm up let us consider first the bifurcations as the coupling c is increased in the case of instantaneous coupling.

The characteristic equation in this case can also be factored into the form (10), where the factor $\Delta_1(\lambda)$ is obtained from (10) by dropping the last term (next to c) and the factor $\Delta_2(\lambda)$ is obtained by substituting $\tau = 0$ in (10).

All three roots of the first factor are real and negative (and independent of c)

$$\lambda_1 = -28.2783, \qquad \lambda_2 = -0.064502, \qquad \lambda_3 = -0.00344965.$$

Let us analyze the roots of the second factor with zero real part. First consider the root $\lambda = 0$. It occurs for

$$c = \frac{3x_0^2+4x_0+4}{2} \approx 2.6527.$$

We shall be mainly interested in the dynamics for far smaller values of c.

Pure imaginary solutions of $\Delta_2(\lambda) = 0$ occur for

$$c_0 \approx 0.674522 \quad \text{and} \quad c_1 \approx 5.17561.$$

Since the stationary solution for $c \in (0, c_0)$ is stable and

$$\left(\frac{d\,\mathrm{Re}\,\lambda}{dc}\right)_{c=c_0} > 0$$

the stationary solution for $c > c_0$ (and $\tau = 0$) is unstable and the bifurcation at $c = c_0$ is destabilizing Hopf bifurcation.

2.4. Delayed coupling $\tau > 0$

Hopf bifurcation curves in the plane (c, τ) are obtained by substituting $\lambda = iv$, where v is real and positive, in the characteristic equation (10). The first and the second factor $\Delta_{1,2}(iv) = 0$ result in

$$c\big(v^2+r^2\big)\big(v^2+1\big)\cos(v\tau) = \mp\big(v^2+r^2\big)\big(Dv^2+E\big) \mp 4r^2\big(v^2+1\big),$$
$$c\big(v^2+r^2\big)\big(v^2+1\big)\sin(v\tau) = \pm v\big[\big(v^2+1\big)\big(v^2+r^2-4r\big) - 10x_0\big(v^2+r^2\big)\big], \tag{11}$$

where

$$E = 3x_0^2 - 6x_0 - c, \qquad D = 3x_0^2 + 4x_0 - c.$$

Squaring and adding the two equations for each factor gives the same result

$$\begin{aligned} &v^{10} + \big(A^2+r^2+1-2k\big)v^8 + \big(A^2r^2+A^2+k^2+r^2-2kr^2-2AB-2k\big)v^6 \\ &\quad + \big(k^2r^2+k^2+A^2r^2+B^2-2ABr^2-2AB-2kr^2\big)v^4 + \big(k^2r^2+B^2-2Br^2-2ABr+2Br^2+2Br\big)v^2 + B^2r^2 \\ &\quad = c^2\big(v^2+r^2\big)^2\big(v^2+1\big)^2, \end{aligned} \tag{12}$$

where

$$A = 3x_0^2 - 6x_0 + 1 + r - c, \qquad B = \big(3x_0^2+4x_0+4-c\big)r,$$

and

$$k = 3x_0^2 r - 6x_0 2 - cr + 3x_0^2 + 4x_0 - c + 5r.$$

As $v^2+r^2 \neq 0$ and $v^2+1 \neq 0$ Eq. (12) can be divided by $(v^2+r^2)(v^2+1)$ resulting in a much simpler bi-qubic equation

$$\omega^3 + \big(A^2-2k-c^2\big)\omega^2 + \big(k^2-2AB-c^2r^2-c^2\big)\omega + B^2 - c^2r^2 = 0, \quad \omega = v^2. \tag{13}$$

This equation has for $c > c_0$ one negative and two positive roots. Both two positive roots, denoted by ω_1 and ω_2, should be substituted, as $v_- = \sqrt{\omega}_1$ and $v_+ = \sqrt{\omega}_2$ (the reason for $\pm$ notation will become clear after formula (26)), in the two equations

obtained by dividing the equations in the two pairs (11) corresponding to the two factors Δ_1 and Δ_2

$$\tau_c(v) = \frac{1}{v}\,\mathrm{ArcTg}\left[\pm\frac{v[(v^2+1)(v^2+r^2-4r)-10x_0(v^2+r^2)]}{(v^2+r^2)(Dv^2+E)\mp 4r^2(v^2+1)}\right]. \tag{14}$$

Writing explicitly different branches of the ArcTg we obtain the following prescription for calculation of the bifurcation values of the time-lag, that can be expressed in the form of two families of formulas. The first family is given by: If

$$\sin(v\tau) = \frac{v[(v^2+1)(v^2+r^2-4r)-10x_0(v^2+r^2)]}{c(v^2+r^2)(v^2+1)} > 0 \tag{15}$$

then

$$\tau_1^j(v) = \frac{1}{v}\left[2j\pi + \arccos\frac{-[(v^2+r^2)(Dv^2+E)+4r^2(v^2+1)]}{c(v^2+r^2)(v^2+1)}\right], \tag{16}$$

and if

$$\sin(v\tau) = \frac{v[(v^2+1)(v^2+r^2-4r)-10x_0(v^2+r^2)]}{c(v^2+r^2)(v^2+1)} < 0 \tag{17}$$

then

$$\tau_1^j(v) = \frac{1}{v}\left[(2j+2)\pi - \arccos\frac{-[(v^2+r^2)(Dv^2+E)+4r^2(v^2+1)]}{c(v^2+r^2)(v^2+1)}\right]. \tag{18}$$

For the second family we have: if (15) is valid than

$$\tau_2^j(v) = \frac{1}{v}\left[(2j+2)\pi - \arccos\frac{(v^2+r^2)(Dv^2+E)+4r^2(v^2+1)}{c(v^2+r^2)(v^2+1)}\right], \tag{19}$$

and if (17) is satisfied than

$$\tau_2^j(v) = \frac{1}{v}\left[2j\pi + \arccos\frac{(v^2+r^2)(Dv^2+E)+4r^2(v^2+1)}{c(v^2+r^2)(v^2+1)}\right]. \tag{20}$$

In the formulas for both families both values $v = v_{1,2} = \sqrt{\omega_{1,2}}$ should be used, and $j = 0, 1, 2, \ldots$.

Formulas (15)–(20) and the two positive roots of (13) are used to draw Hopf bifurcation curves in Fig. 1(a).

The sign of the Hopf bifurcation on each of the critical curves is determined as follows. From the characteristic equation (10) we have

$$\left[\frac{\partial\Delta_1}{\partial\lambda}\frac{d\lambda}{d\tau} + \frac{\partial\Delta_1}{\partial\tau}\right]\Delta_2 + \Delta_1\left[\frac{\partial\Delta_2}{\partial\lambda}\frac{d\lambda}{d\tau} + \frac{\partial\Delta_2}{\partial\tau}\right] = 0, \tag{21}$$

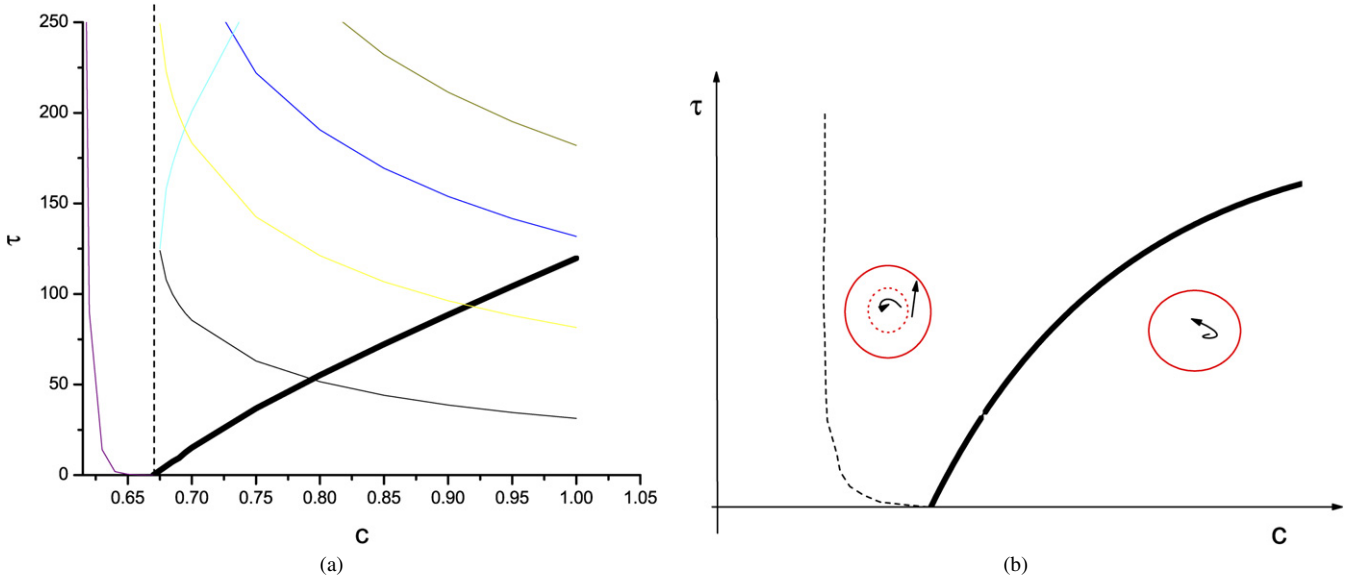

Fig. 1. Illustrates bifurcations relevant for the dynamics near the stationary solution. (a) Curves on the right of the dashed vertical are Hopf bifurcations given by formulas (15)–(18) of the stationary solution, and the curve on the left is the curve of the fold limit cycle bifurcations; (b) qualitative picture of the dynamics near the fold limit cycle and the first subcritical Hopf (thick) bifurcation curves.

or

$$\frac{d\lambda}{d\tau} = \frac{\frac{\partial \Delta_1}{\partial \tau}\Delta_2 + \frac{\partial \Delta_2}{\partial \tau}\Delta_1}{\frac{\partial \Delta_1}{\partial \lambda}\Delta_2 + \frac{\partial \Delta_2}{\partial \lambda}\Delta_1}. \tag{22}$$

Thus,

$$\operatorname{sgn}\left[\frac{d\operatorname{Re}\lambda}{d\tau}\right]_{\tau=\tau_c} = \operatorname{sgn}\left[\operatorname{Re}\left(\frac{d\lambda}{d\tau}\right)^{-1}\right]_{\tau=\tau_c} = \operatorname{sgn}\left[\frac{3v^4 + 2(A^2 - 2k - c^2)v^2 + k^2 - 2AB - c^2r^2 - c^2}{c^2(v^2+1)(v^2+2)}\right]. \tag{23}$$

To proceed it is useful to notice that the characteristic equation (13) with the substitution $\omega = v^2$ can be used to rewrite the last expression in the following form

$$\operatorname{sgn}\left[\frac{\phi'(\omega)}{c^2(\omega+1)(\omega+r^2)}\right], \tag{24}$$

where ϕ is the following function

$$\phi(\omega) = \omega^3 + \left(A^2 - 2k - c^2\right)\omega^2 + \left(k^2 - 2AB - c^2r^2 - c^2\right)\omega + B^2 - c^2r^2. \tag{25}$$

An analysis of the third order polynomial $\phi(\omega)$ shows that $\phi'(\omega_1) < 0$ and that $\phi'(\omega_1) > 0$ from which it follows that

$$\left(\frac{d\operatorname{Re}\lambda}{d\tau}\right)_{\tau_{c,+}} > 0, \qquad \left(\frac{d\operatorname{Re}\lambda}{d\tau}\right)_{\tau_{c,-}} < 0, \tag{26}$$

where $\tau_{c,\pm} \equiv \tau^j_{1,2}(v_\pm)$, $j = 0, 1, 2, \ldots$. This analyzes shows which of the Hopf bifurcations on curves like in Fig. 1 increases or decreases the number of local unstable directions [10].

In order to complete the bifurcation picture we consider numerically what happens for $c < c_0$ when the time lag τ is increased. For $c < c_0$ and any τ the stationary state is stable, but numerical evidence shows that there is relatively small interval of c just below c_0 such that there is also a stable limit cycle provided that τ is large enough. Thus, for such values of c and sufficiently large τ a flip bifurcation occurs and the stable and an unstable limit cycles appear. Further numerical evidence shows that the critical values of τ for this bifurcation to occur go to zero as c approaches c_0 from below. Furthermore, the curve of this critical values $\tau_c(c)$, $c < c_0$ approaches $\tau = 0$ tangentially to the c axes. This is illustrated in Fig. 1(a), (b). Thus, for $c < c_0$ there is the stable stationary solution and possibly, if c is not far from c_0 and if τ is large enough, the stable limit cycle. As c is increased for fixed and small $\tau > 0$ the system crosses the bifurcation curve $\tau_{1,-}$ and the reversed subcritical Hopf bifurcation occurs. The unstable limit cycle collapses onto the stationary point and destabilizes it. The stable limit cycle remains stable. As the result, for $\tau < \tau^0_{1,-}$ (bold type curve in Fig. 1(a), (b)) and $c > c_0$ there is only the stable limit cycle attractor. On the other hand, for fixed c slightly larger than c_0 as τ is increased the system crosses the bifurcation curve $\tau^0_{1,-}$, the subcritical Hopf bifurcation occurs, the stationary solution becomes stable and an unstable limit cycle is born. Thus the system is again in the domain where it is bistable with the stable stationary solution and the stable limit cycle. Further increase of τ beyond the next bifurcation curve destabilizes the stationary state but the limit cycle remains stable.

3. Bursting and synchronization

If the coupling constant c is sufficiently large the system, in general, displays the bursting behavior. The properties of bursts, like the frequency of their occurrence and the number of spikes in each burst, depend on the value of the time-lag. The periods of bursting and the dynamics in such periods for the two neurons are synchronous for the coupling parameter c and the time-lag τ in a certain domain. In this section we report some of the results of our numerical study of the properties of bursts and their synchronization. The results will be presented by commenting Figs. 2–4.

Bifurcation analyzes, presented in the last section, suggests that the bursting dynamics occurs in general for such values of (c, τ) that imply instability of the stationary solution. The bursts in the dynamics of the fast (x, y) system occur for such (c, τ) that imply oscillatory behavior of the slow variable z, and in particular during the periods when $dz/dt > 0$. For such (c, τ) the bursting orbits represent, in general, the only attractor. However, there is a small domain of (c, τ) values when, besides the bursting orbits, the stationary solution has relatively small domain of initial states attracted to it. In this case the system is bistable. Near the boundaries of this domain, since they are determined by the Hopf bifurcation of the stationary solution, the system starting from an initial state near the stationary state could oscillate for a long time with a small amplitude near the stationary state before it converges to the attractor corresponding to the bursting dynamics. This is illustrated in Fig. 2.

The dependence of the properties of bursting on the coupling c and the time-lag τ is illustrated in Fig. 3. Once the coupling is strong enough for bursting to occur, i.e. $c > c_0$, the frequency of the bursts depends very little on the coupling c. However, the number of spikes in each burst depends on c. On the other hand, the frequency of bursts very much depends on the time-lag. This

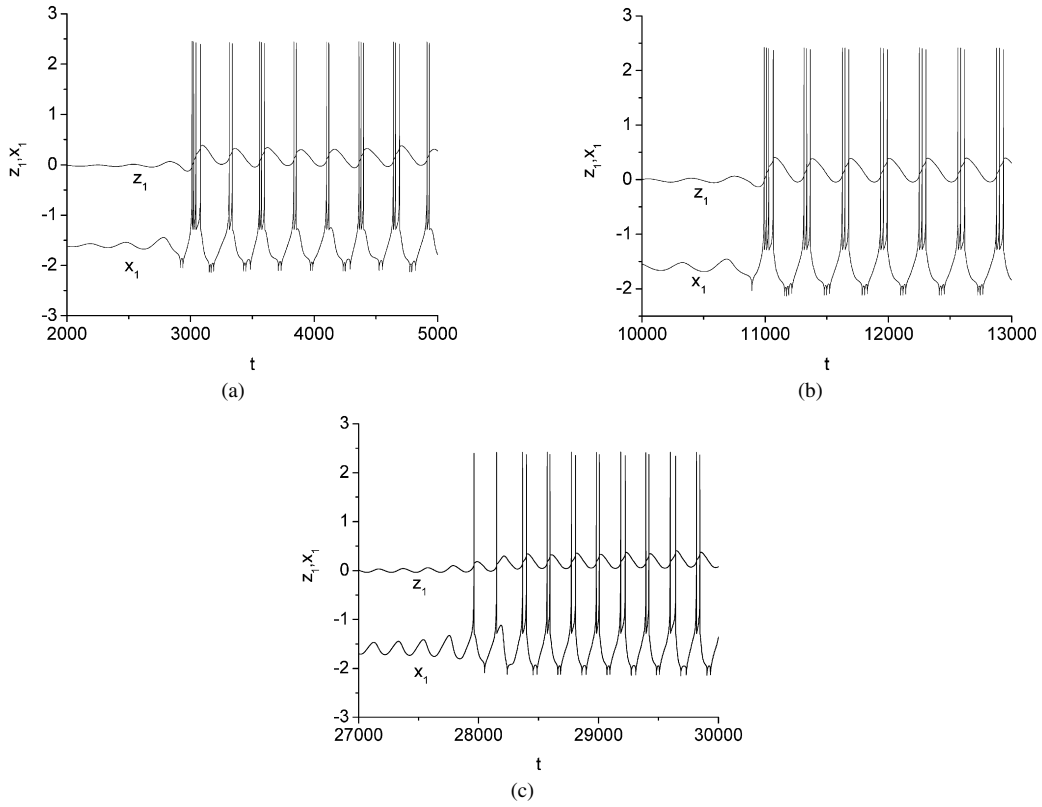

Fig. 2. Illustrates time series $x_1(t), z_1(t)$ for the orbits that start close to the stationary solution and converge onto the bursting dynamics: (a) $(c, \tau) = (0.7, 0)$ close to $(c_0, 0)$; (b) $(c, \tau) = (0.7, 12)$ just below the first curve of subcritical Hopf bifurcations; (c) $(c, \tau) = (0.7, 88)$ just above the second curve of Hopf bifurcations. For the values of τ in between the stationary solution is stable.

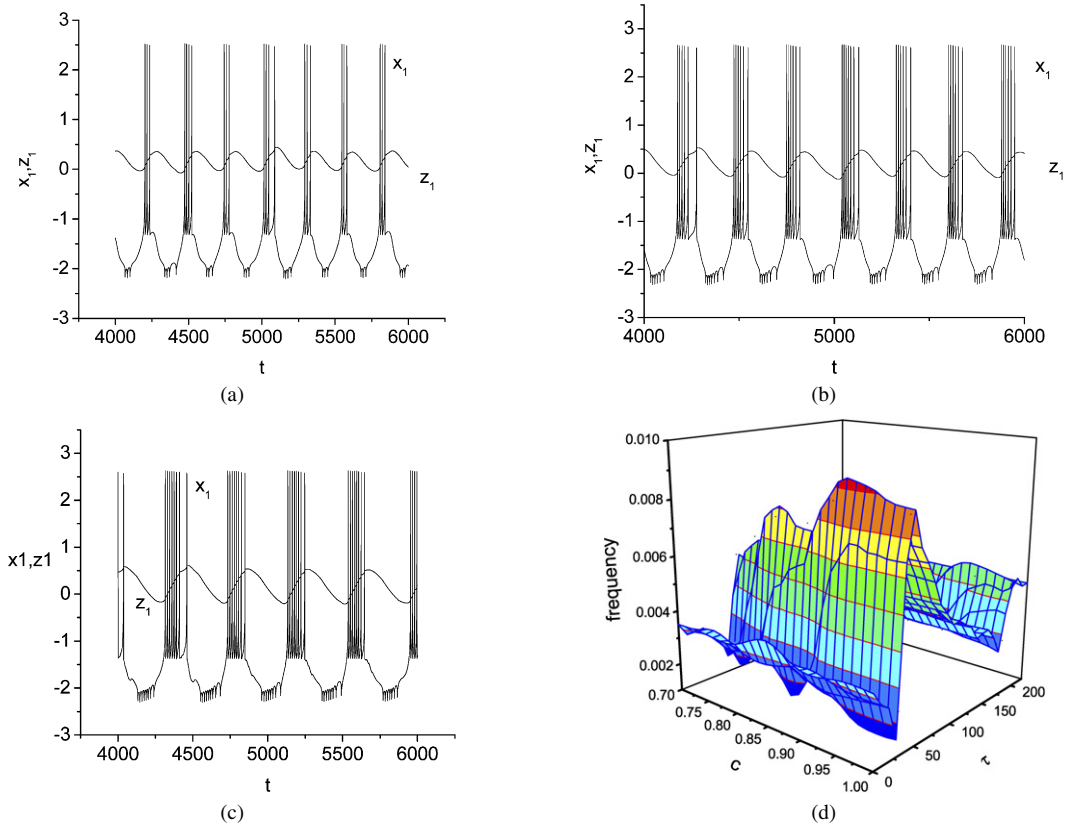

Fig. 3. Illustrates the dependence of the frequency of bursts on c and τ. Values of (c, τ) are: (a) $(c, \tau) = (0.8, 0)$, (b) $(c, \tau) = (1, 0)$, (c) $(c, \tau) = (1, 25)$.

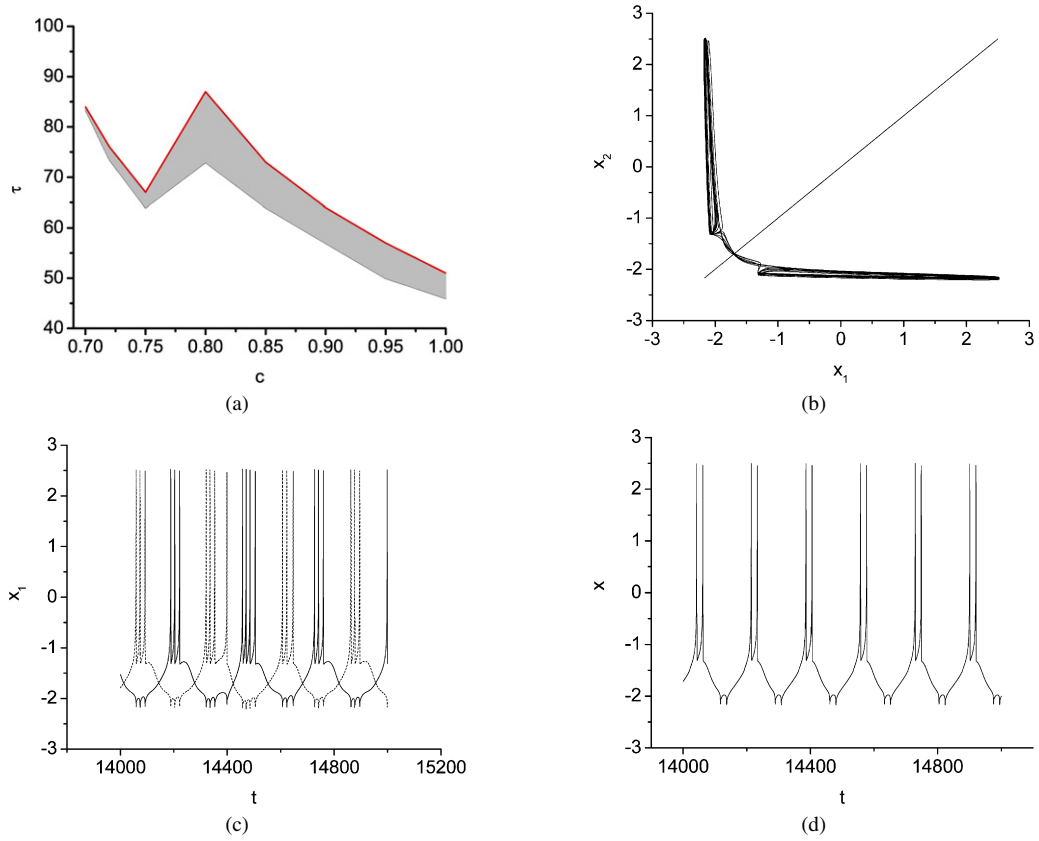

Fig. 4. Illustrates synchronization by time-delay. (a) Domain of (c, τ) with exactly synchronous dynamics is illustrated by the shaded region; (b) projections of the attractors on (x_1, x_2) planes for asynchronous dynamics corresponds to $(c, \tau) = (0.8, 0)$ and the synchronous to $(c, \tau) = (0.8, 75)$, (c) time series $(x_1(t), x_2(t))$ for $(c, \tau) = (0.8, 0)$, (d) time series $(x_1(t), x_2(t))$ for $(c, \tau) = (0.8, 75)$.

dependence is in general not smooth, but is dominated by large jumps which occur for certain values of τ. This global bifurcation, resulting in the frequency jumps, is not related to the Hopf bifurcations of the stationary solution studied in the previous section.

Synchronization of bursting in instantaneously coupled HR neurons was studies long time ago in the seminal paper by Abarbanel, Huerta, Rabinovich, Rulkov, Rowat and Selvestron [6]. There, it was shown that sufficiently strong coupling leads to exact synchronization of bursting. However, the values of the coupling that induce the synchronization are estimated numerically to be unrealistically large. Much later Dhamala, Jirsa and Ding [9] have demonstrated numerically that time-lag in the electric coupling enhances the synchronization so that it can occur for much smaller values of c than in the instantaneous coupling. They analyzed synchronization of bursting in HR neurons like in (2) but with the external current I set to the value which implies the bursting of each neuron even with the zero coupling. We have analyzed the synchronization of HR neurons with the external current $I = 0$, so that the bursting is introduced by coupling. It turns out that as soon as the bursting occurs for $c > c_0$ there is also a domain of values of the time-lag for which the exactly synchronous dynamics is stable. Estimates of the largest Lyapunov exponent transversal to the synchronization manifold and of the correlation between the components of the two neurons are used to quantitatively study the stability of the exactly synchronous solution. Applications of both methods to DDEs have been described in details elsewhere (see for example [9,11,12]) and need not be repeated here. The results are illustrated in Fig. 4. Numerical evidence supports the conclusion that for the indicated values of (c, τ) the exactly synchronous dynamics is globally stable. We are confident that sufficient numerical test to claim the global stability even in the case of an infinite-dimensional system like (2) have been performed. Consistently with the intuition, the domain of τ for which the bursting is exactly synchronous is smallest for c near c_0, and the domain moves to the smaller values of τ as c is sufficiently increased. However the largest domain of τ that imply synchronization occurs for intermediate values of $c \approx 0.8$.

4. Summary and discussion

We have analyzed stability and bifurcations of the stationary solution and the exact synchronization of the bursting dynamics for the pair of delayed coupled HR neurons. Bifurcation analyzes shows that the instantaneous coupling can introduce instability of the stationary solution and numerical results show that the this coupling leads to the bursting dynamics. Further result of the bifurcation analyzes shows that there is a domain of the values of time-lag τ away from zero such that the stationary solution is stable when τ is in this domain and is unstable for τ below and above this domain. Numerical evidence shows that for such c and τ the system is

bi-stable with the stable stationary solution and the bursting dynamics as the two attractors. Dependence of the frequency of bursts on the time-lag τ and the coupling c is studied for a range of values of (c, τ). It is shown that exactly synchronous bursting dynamics is possible for all values of the coupling that imply the bursting, provided that the time-lag is in the corresponding domain.

It should be interesting to study systems with larger number of delayed coupled HR neurons, possibly with an additive or multiplicative noise that could play an important role. Preliminary calculations indicate that in chains of nearest neighbors delayed coupled units nonhomogeneous spatial patterns of synchronization are possible. Also, the noise could have quite different qualitative effects on the deterministic dynamics depending on the domain of time-lags and the values of the coupling.

Acknowledgements

This work is partly supported by the Serbian Ministry of Science contract No. 141003. N.B. should also like to acknowledge the support and hospitality of the Abdus Salam ICTP.

References

[1] N. Burić, D. Todorović, Phys. Rev. E 67 (2003) 066222.
[2] E.M. Izhikevich, Int. J. Bifur. Chaos 10 (2000) 1171.
[3] N. Burić, I. Grozdanović, N. Vasović, Chaos Solitons Fractals 23 (2005) 1221.
[4] N. Burić, D. Todorović, Int. J. Bifur. Chaos 15 (2005) 1775.
[5] J.L. Hindmarch, R.M. Rose, Proc. R. Soc. London Ser. B 221 (1984) 87.
[6] H.D.I. Abarbanel, et al., Neural Comput. 8 (1996) 1567.
[7] R.M. Ghigliazza, P. Holms, SIAM J. Appl. Dynam. Systems 3 (2004) 636.
[8] X.-J. Wang, Physica D 62 (1993) 263.
[9] M. Dhamala, V.K. Jirsa, M. Ding, Phys. Rev. Lett. 92 (2004) 074104.
[10] J. Hale, S.V. Lunel, Introduction to Functional Differential Equations, Springer-Verlag, New York, 1993.
[11] K. Pyragas, Phys. Rev. E 58 (1998) 3067.
[12] N. Burić, K. Todorović, N. Vasović, Int. J. Bifur. Chaos 16 (2006) 1569.